148.

U. RADIO EMISSION FROM QUIESCENT FILAMENTS

KENNETH R. LANG
TUFTS UNIVERSITY

IAU COLLOQUIUM No. 117
DYNAMICS OF PROMINENCES

Hvar, Yugoslavia

September 25-29, 1989

ABSTRACT

Full-disk VLA synthesis maps of the quiet Sun indicate that filaments can be seen in emission at 91.6-cm wavelength; they are detected in absorption at shorter microwave wavelengths. The 91.6-cm emission has a brightness temperature of $T_B = 3 \times 10^5$ K. It is hotter, wider and longer than the underlying filament detected at Hα wavelengths, but the similarity between the shape, position, elongation and orientation of the radio and optical features suggests their close association. The 91.6-cm emission is attributed to the thermal bremsstrahlung of a hot transition sheath that envelopes the Hα filament and acts as an interface between the cool, dense Hα filament and the hotter, rarefied corona. The transition sheath is seen in emission because of the lower optical depth of the corona at 90-cm wavelength, and the width of this sheet is 10^9cm. A power law gradient in pressure provides a better match to the observations than a constant pressure model; definitive tests of theoretical models await simultaneous multi-wavelength studies of filaments at different observing angles. When the thermal bremsstrahlung is optically thin, the magnetic field strength in the transition sheath can be inferred from the observed circular polarization. Variable physical parameters of the sheath, such as width, electron density, and electron temperature, can explain controversial reports of the detection of, or the failure to detect, the meter-wavelength counterpart of Hα filaments.

Subject headings: Sun: filaments - Sun: prominences - Sun: radio radiation
Sun: coronal loops - Sun: magnetic fields

I. INTRODUCTION

Filaments are cooler than the surrounding corona, and therefore appear as depressions in the quiet Sun background at centimeter wavelengths (Gary, 1986; Kundu, Melozzi and Shevgaonkar, 1986); the cool filaments can also appear as depressions at millimeter wavelengths (Schmahl, Bobrowksy and Kundu, 1981). Regions that overlie filaments can now be detected using the VLA at the longer 91.6-cm wavelength; the higher temperatures produce regions of increased emission when compared with the surrounding quiet Sun background.

Previous observations have, however, led to an ongoing controversy about the optical counterparts of the quiescent, or non-flaring, solar radiation at meter wavelengths. A statistical study of numerous one-dimensional Nancay scans suggested that many quiescent meter-wavelength sources are associated with filament corridors as seen on Hα synoptic maps (Axisa et al., 1971), but subsequent two-dimensional maps indicated that most filaments have no radio counterpart at meter wavelengths (Alissandrakis, Lantos and Nicolaidis, 1985; Lantos et al., 1987).

The VLA provides an order-of-magnitude improvement in angular resolution over all previous meter-wavelength investigations of the quiet Sun and might therefore help resolve this controversy. The first VLA observations of the quiescent coronal at 92-cm wavelength indicated no systematic association of any of the radio sources with any optical counterpart, including active regions, filaments, sunspots and the magnetic neutral line in the underlying photosphere (Lang, Willson, and Trottet, 1987). Full disk VLA observations by Shevgaonkar, Kundu, and Jackson (1988) indicated that the 90-cm sources may be indentified as streamers above Hα filaments. However, our comparison of

their data with Hα observations (Solar Geophysical Data) indicates that many of the intense 90-cm sources do not overlie Hα filaments.

One probable source of confusion is noise storms, the most common form of solar activity at meter wavelengths. The numerous type I bursts and background continuum of noise storms have been associated with coronal loop structures detected during Skylab at soft X-ray wavelengths (Stewart and Vorpahl, 1977; Gergely, Kundu, Golub and Webb, 1980) as well as with large-scale EUV loops (Stewart, Brueckner and Dere, 1986). VLA observations at 91.6-cm wavelength confirm the location of noise storms in large-scale magnetic loops that either overlie coronal loops within individual active regions of connect these regions with more distant areas on the Sun (Lang and Willson, 1987); such conclusions were also anticipated by metric wavelength observations with the Nancay Radioheliograph (Lantos-Jarry, 1970; Mercier et al., 1984). Detection of the meter-wavelength counterpart of filaments requires observations when the intense noise storms are not present.

In this paper we present VLA 91.6-cm synthesis maps during quiescent periods without any noise storm activity. In Section II we show that there is an excellent association of some 91.6-cm sources with Hα filaments. The radio filaments are enhanced over the surrounding quiescent emission, rather than depressed. Not all Hα filaments, however, exhibit detectable 91.6-cm counterparts. In Section III we interpret some quiescent 91.6-cm sources in terms of the thermal radiation of a sheath overlying a Hα filament, and with temperatures intermediate between those of its Hα counterpart and the surrounding corona.

II. OBSERVATIONS

The Sun was observed with the VLA in the C/D hybrid configuration between 1315 and 1610 UT on 15 May 1988 using 27 antennas at 20.7-cm wavelength (1446 MHz) and 19 antennas at 91.6-cm wavelength (327.5 MHz) with respective bandwidths of 12.5 and 3.125 MHz. The full-disk synthesis maps at 20.7-cm are given elsewhere (Lang and Willson, 1989a), where they are used to identify active regions that interact via large-scale, trans-equatorial magnetic loops. Here we focus on the full-disk 91.6-cm synthesis map shown in Figure 1 (left). Although all four Stokes parameters were sampled, there was no detectable circular polarization, so our three-hour synthesis map refers to the total intensity, I. Burst data have been removed prior to making this synthesis map. The details of calibration procedures are given in Lang and Willson (1989b).

The contours of the resulting map (Figure 1, left) mark levels of equal brightness temperature, T_B, with an outermost contour of $T_B = 7.8 \times 10^4$ K, a contour interval of 7.8×10^4 K, and peak brightness tempeature of $T_B = 7.8 \times 10^5$ K. The mean brightness temperatures of the elongated sources marked A and B are, for example, estimated to Be $T_B \sim 3 \times 10^5$ K above the surrounding quiet Sun level of $T_B \sim 4 \times 10^5$ K, with an uncertainty of 20 percent.

An Hα photograph taken on the same day (15 May 1988) is also shown in Figure 1 (right); it contains several dark, elongated filaments. Two of these have counterparts in the 91.6-cm map with similar shapes, positions, elongations and orientations; they are designated by the letters A and B in the 91.6-cm map. The smaller filaments seen in the north-central regions also seem to have 91.6-cm counterparts, but there is no increased 91.6-cm emission in the vicinity of the dark filaments that lie near the north-east an south-east limbs (marked C and E on the 91.6-cm map).

The intense 91.6-cm emission detected near the equator on the east limb (marked D) may be due to a coronal streamer. Sacramento Peak coronagraph data (Solar Geophysical Data) show coronal material in this region, as well as those that have no detectable 91.6-cm radiation. No underlying active regions or filaments were visible as the Sun rotated and the limb region turned in to view during the following days.

Depressions in the 91.6-cm radiation are found in the central equatorial regions (hatched regions). They may be at least partly due to coronal holes, but the only available He 10830 data, taken on 14 May, do not exhibit a detectable equatorial coronal hole. Examination of the 91.6-cm maps for shorter time scales showed no evidence for variable features on time scales of a few tens of minutes.

III. DISCUSSION

The similarity in shape, position, elongation and orietation strongly suggests that the radio emision from soucres A and B is associated with the underlying dark filaments detected in the Hα photograph, but the radio emission could also be associated with bright Hα plage and their associated higher magnetic fields. The most intense emission from source A coincides with a dark filament rather than plage, and the most intense part of source B corresponds to the largest part of the underlying filament. Moreover, the weaker emission from both sources has the same shape and orientation as the associated narrow, elongated filaments. We therefore attribute the radio emission to these filaments, whle noticing that Hα plage might also play a role in enhanced 91.6-cm emission.

We therefore interpret the regions of increased 91.6-cm emission around filaments (sources A and B) in terms of a hot sheath that envelops the cooler Hα filaments; such a surrounding sheath is suggested by the fact that the radio wavelength features are similar in shape to, but wider, longer and hotter than, their optical counterparts. The mean 91.6-cm brightness temperatures of $T_B \sim 3 \times 10^5$ K, for example, lie between the electron temperatures of the cool Hα filaments and the electron temperature of the surrounding corona.

In order to gain a quantitative view of the transiton sheath, we compare our observations with the data and models given by Kundu, Melozzi and Shevgaonkar (1986). Their VLA observations at the shorter 6 and 20 cm wavelengths indicated radio depressions above Hα filaments, in comparison with the hot surrounding corona, but a transition sheath was indicated by the fact that the radio filaments are larger in size than their optical counterparts and that the brightness temperature, T_B, of the radio filaments

increases with wavelength from $T_B \sim 1.5 \times 10^4$ K at 6 cm to $T_B \sim 5 \times 10^4$ K at 20 cm. Our higher brightness temperature of $T_B \sim 3 \times 10^5$ K at the longer 91.6-cm wavelength can be explained by the larger optical depth of thermal bremsstrahlung from the transition sheath at longer wavelengths, and the fact that the 91.6-cm sheath is seen in emission can be explained by the relatively low optical depth of the low-density corona. The brightness temperature contribution of the corona has been taken into account by subtracting the background solar disk temperature in obtaining our filament brightness temperature of $T_B \sim 3 \times 10^5$K. If the transition sheath is observed as optically thin bremsstrahlung during future observations, the magnetic field strength can be inferred from the observed circular polarization.

We have assumed that the variation of temperature with height in the transition sheath is that given by Kundu, Melozzi and Shevgaonkar (1986); their data resulted from an assumed balance between the thermal energy conducted in from the corona and the energy radiated away. These temperatures, T, were then combined with three pressure models to infer the electron density, N, and the equation of transfer was solved assuming free-free emission with these values of temperature and density. The three models were a constant pressure model $P = NT = 3 \times 10^{14}$ cm^{-3} K, and two power law models $P = NT = aT^n$, with $a = 2.5 \times 10^{17}$, $n = -0.58$ and $a = 4 \times 10^{17}$, $n = -0.62$. The calculated brightness temperatures of these two models are shown in Figure 2 together with our measurements at 91.6 cm and those of other observers at shorter wavelengths. This figure indicates that the brightness temperature of the constant pressure model is too high at both 20 cm and 90 cm, with respective values of $T_B \sim 9 \times 10^4$ K and $T_B \sim 6 \times 10^5$ K. The power law models are more in accord with the observational data; at 20 cm

and 90 cm they both produce respective values of $T_B \sim 5 \times 10^4$ K and $T_B \sim 3 \times 10^5$ K. Also note that the 20 cm point is an average of several observations for different observing angles, so this difference cannot account for the result. Detailed model comparisons await future multi-wavelength studies of the same filament at the same time for different observing angles.

So, the observed 91.6-cm structures that are associated with these Hα filaments may be interpreted as the thermal bremsstrahlung of a hot (electron temperature $T_e \approx 3 \times 10^5$ K) sheath that envelops a Hα filament. Such a sheath acts as the boundary between the filament and the surrounding million-degree corona. A loop thickness of $L \approx 10^9$ cm, or about one fiftieth of the $10' \approx 5 \times 10^{10}$ cm extent of the radio sources A and B, has been inferred by deconvolving the observed radio width, to take into account the beamwidth, and using the convolution relation to subtract the observed width of the Hα filament. Such a thickness is consistent with the models of Kundu, Melozzi and Shevgaonkar (1986). If the hypothesized sheath were substantially thinner than the assumed thickness of $L \approx 10^9$ cm, then the optical depth for thermal bremsstrahlung would be much smaller, and the optically-thin sheath might not be detectable. And if the electron density of the sheath was only slightly higher, then its plasma frequency would exceed our observing frequency, and the sheath radiation could not propagate out to be observed. Variable physical parameters of the sheath might therefore easily explain why the elusive meter-wavelength counterpart of Hα filaments is only sometimes observed; just the right thickness, electron density and electron temperature are required for detection.

ACKNOWLEDGMENTS

Radio astronomical studies of the Sun at Tufts University are supported under grant AFOSR-89-0147 with the Air Force Office of Scientific Research. The Very Large Array is operated by Associated Universities, Inc., under contract with the National Science Foundation. The data presented in this paper were taken during collaborative long-wavelength solar observations by Tufts University and the Observatoire de Paris - Meudon, under the support of National Science Foundation grant INT-8602285 and Centre National de la Recherche Scientfique grant 920038.

REFERENCES

Alissandrakis, C.E., Lantos, P., and Nicolaidis, E. 1985, Solar Phys., 97, 267.

Axisa, F., Avignon, Y., Martres, M.J., Pick, M., and Simon, P. 1971, Solar Phys., 19, 110.

Gary, D.E. 1986, in Coronal and Prominence Plasmas, ed. A.I. Poland (NASA Conf. Pub. 2442), p. 121.

Gergely, T.E., and Kundu, M.R. 1980, in Radio Physics of the Sun. IAU Symposium No. 86, ed. M.R. Kundu and T.E. Gergely, p. 435.

Kundu, M.R., Melozzi, M., and Shevgaonkar, R.K., 1986, Astron. Ap., 167, 166.

Lang, K.R., and Willson, R.F. 1987, Ap.J., 319, 514.

Lang, K.R., and Willson, R.F. 1989a, Ap. J. (Letters) 344, L 77.

Lang, K.R., and Willson, R.F. 1989b, Ap. J. (Letters) 344, L 73.

Lang, K.R., Willson, R.F., and Trottet, G. 1988, Astron. Ap., 199, 325.

Lantos, P., Alissandrakis, C.E., Gergely, T., and Kundu, M.R. 1987, Solar Phys., 112, 325.

Lantos - Jarry, M.F. 1970, Solar Phys., 15, 40.

Mercier, C., Elgaroy, O., Tiamicha, A. and Zlobec, P. 1984, Solar Phys., 92, 375.

Schmahl, E.J., Bobrowksy, M., and Kundu, M.R. 1981, Solar Phys., 71, 311.

Stewart, R.T., Brueckner, G.E., and Dere, K.P. 1986, Solar Phys., 106, 107.

Stewart, R.T., and Vorpahl, J. 1977, Solar Phys., 55, 111.

FIGURE LEGENDS

FIG. 1. A three-hour Very Large Array (VLA) synthesis map of the total intensity, I, from the visible solar disk at 91.6-cm (left) is compared with an Hα photograph (right) taken at Boulder Solar Observatory - at 1415 UT on the same day (15 May 1988, courtesy of Pat McIntosh). The synthesized beamwidth is denoted by the small black spot in the lower right-hand corner; it has angular dimension of 80" x 55" at a position angle of -20^{o}. The circle in the 91.6-cm map denotes the visible solar limb, and the tick marks denote solar north and south. Radio wavelength emission from dark, elongated filaments in the Hα photo are designated by A and B in the 91.6-cm map. Filaments C and E did not correspond to enhanced 91.6-cm emission while source D probably coincides with a coronal streamer. The hatched regions in the central equatorial regions correspond to depressions in the 91.6-cm emission.

FIG. 2. Calculated brightness temperatures for a constant pressure $P = 3 \times 10^{14}$ cm^{-3} K (dashed line) and a power law pressure $P = 2.5 \times 10^{17}$ $T^{-0.58}$ with $dT/dh = 0$ at height $h = 0$. The observed temperature at 91.6-cm (filled circle) is from this paper, whereas the other values (crosses, open circles, open squares and open triangles) are from Kundu, Melozzi and Shevgaonkar (1986) with their 6 and 20 cm measurements increased by a Factor of 1.7 due to the detection of a software calibration error. The brightness temperatures refer to mean values over the radio source.

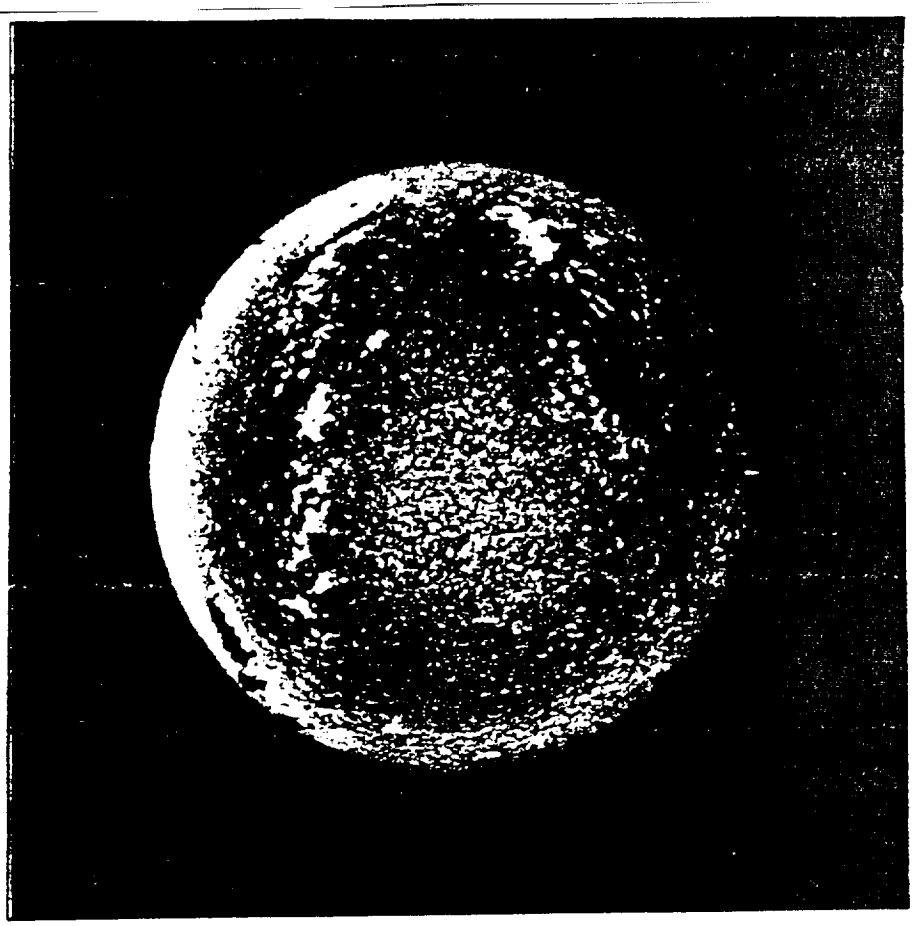

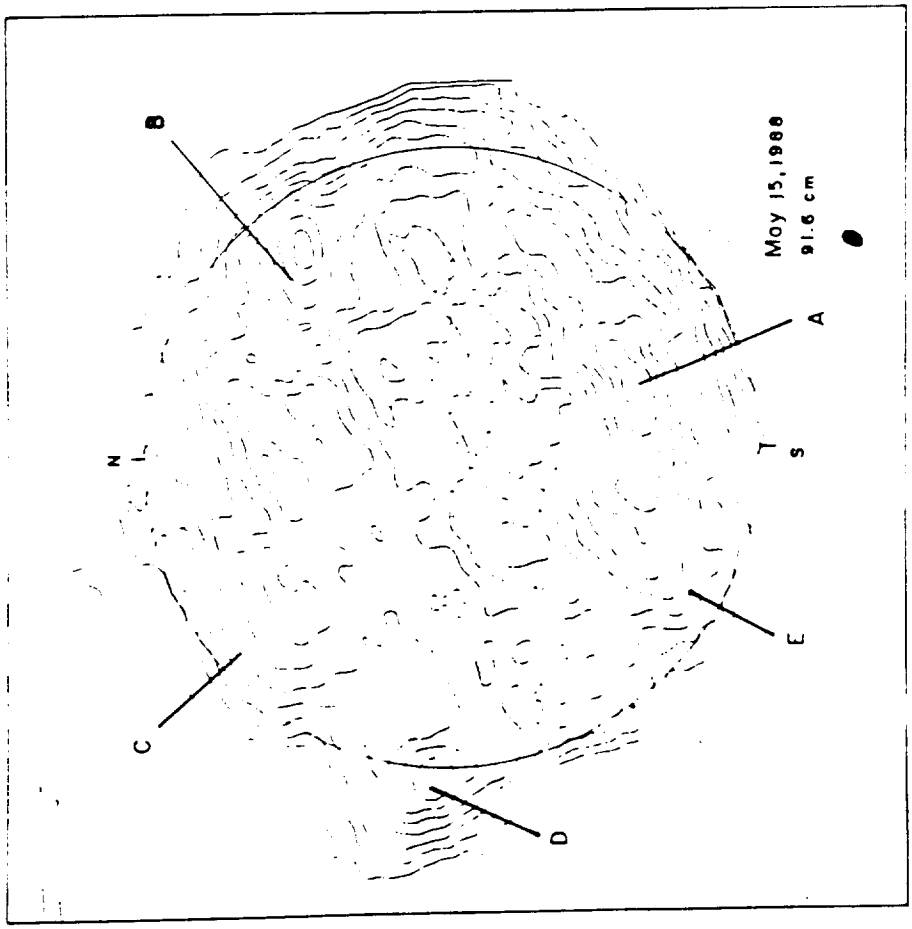

ORIGINAL PAGE IS
OF POOR QUALITY

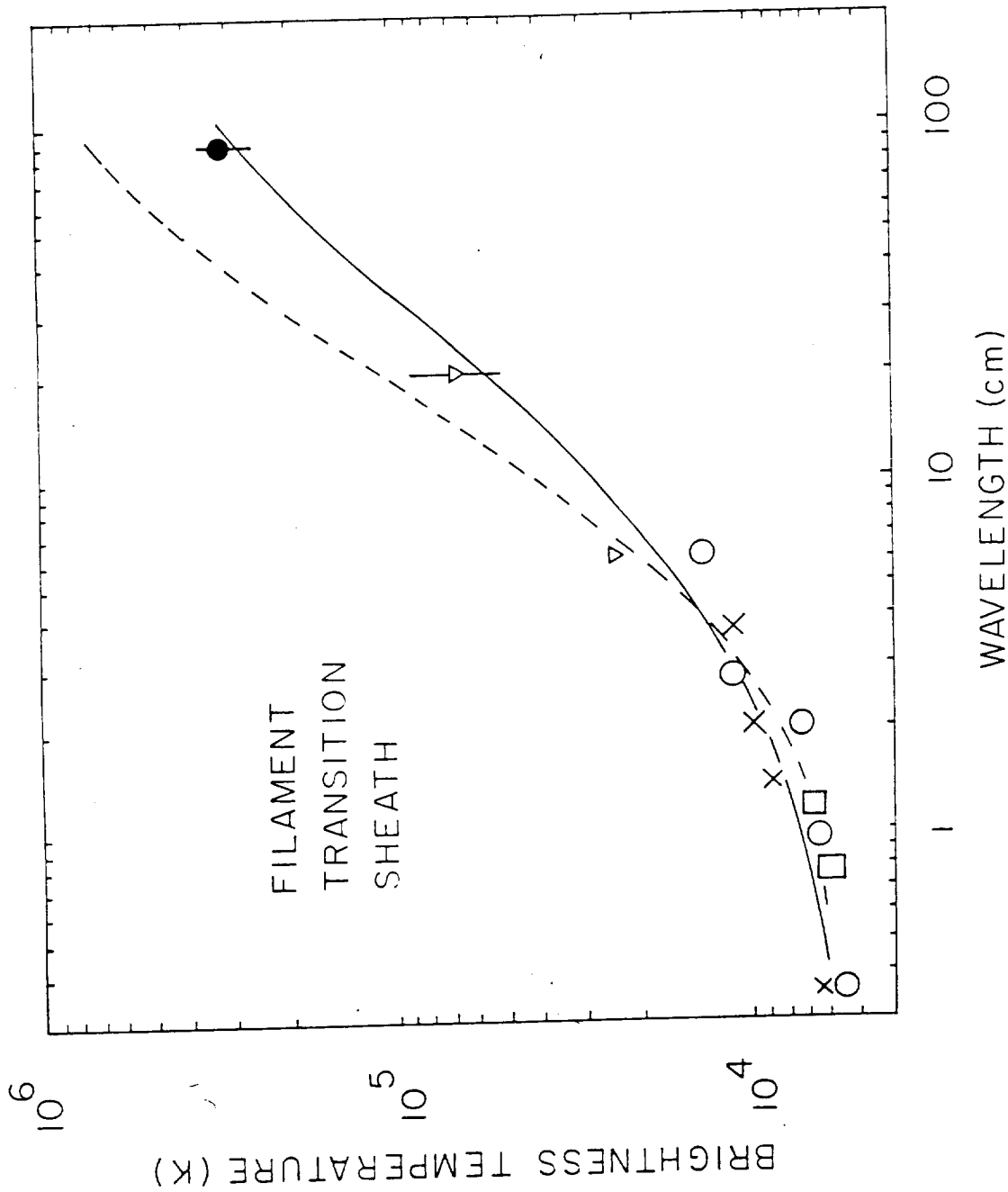
BRIGHTNESS TEMPERATURE (K)
10^6
10^5
10^4
FILAMENT
TRANSITION
SHEATH
1
10
100
WAVELENGTH (cm)